
Laser Diode to Single-Mode Fiber Coupling Efficiency: Part 1 - Butt Coupling

Justin D. Redd, Ph.D.

Published by Maxim Integrated Products as application note HFAN-2.0.2
<https://pdfserv.maximintegrated.com/en/an/AN1816.pdf>

Laser Diode to Single-Mode Fiber Coupling Efficiency: Part 1 - Butt Coupling

1 Introduction

For fiber-optic transmitters, it is generally desirable to utilize the optical power generated by the laser diode as efficiently as possible. In practice, more than half of this power may be lost at the interface between a laser diode and a single-mode optical fiber. The purpose of this application note is to analyze the primary mechanisms that contribute to loss of efficiency.

Butt coupling is the most basic method of coupling the optical output from a laser diode into an optical fiber. This simply consists of placing the cleaved end of the fiber as close as possible to the output aperture of the laser diode. In addition to butt coupling, there are other (more complex) methods of coupling, but these are outside the scope of this application note.

There are many types of optical fiber in use today, including multimode, graded index, dispersion shifted, etc., and each has advantages for specific applications. For purposes of this analysis, we will use the published characteristics of Corning SMF-28 step index fiber, which is one of the most widely used single-mode optical fibers. For this fiber, the numerical aperture (equivalent to the acceptance angle in units of radians) is 0.14, the core index of refraction is 1.650, the cladding index of refraction is 1.644, the core diameter is $8.2\mu\text{m}$, and the cladding diameter is $125\mu\text{m}$.

2 Reflection and Refraction at the Air-Glass Boundary

When light is incident on the boundary between one medium and another, part of it will be reflected away from the boundary and the rest will be transmitted across the boundary and into the new medium. The light that is transmitted into the new medium will generally experience a change in direction due to refraction. This is illustrated in Figure 1.

The incident, reflected, and transmitted light components shown in Figure 1 all travel in the same

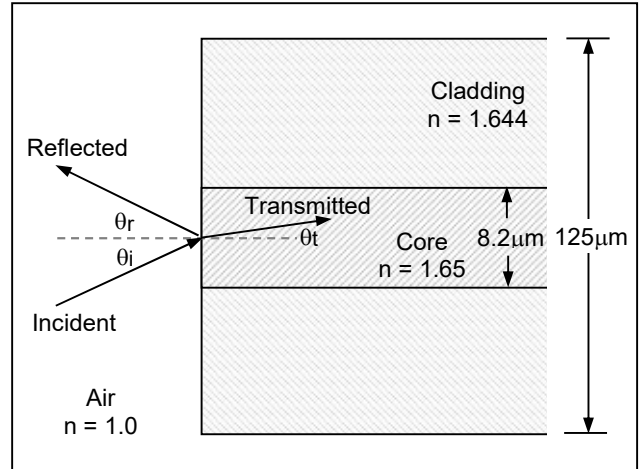


Figure 1. Light incident on an air-glass boundary

two-dimensional plane. The angle of incidence, θ_i , and the angle of reflection, θ_r , are equal. The angle of the transmitted light, θ_t , relative to the normal at the boundary, is related to the angle of incidence by Snell's law:

$$n_1 \sin \theta_1 = n_2 \sin \theta_2 \quad (1)$$

where n_1 and n_2 are the indices of refraction for the incident and transmitting media, respectively, $\theta_1 = \theta_i = \theta_r$, and $\theta_2 = \theta_t$.

The fraction of the incident light amplitude that is reflected can be calculated using the Fresnel equations:

$$R_{TE} = \left| \frac{n_1 \cos \theta_1 - n_2 \cos \theta_2}{n_1 \cos \theta_1 + n_2 \cos \theta_2} \right| \quad (2)$$

$$R_{TM} = \left| \frac{n_2 \cos \theta_1 - n_1 \cos \theta_2}{n_2 \cos \theta_1 + n_1 \cos \theta_2} \right| \quad (3)$$

where R_{TE} and R_{TM} represent the amplitude reflection coefficients (i.e., the ratios of the reflected to the incident amplitudes) for the transverse electric and transverse magnetic polarizations of the incident



light relative to the plane of the boundary. The amplitude reflection coefficients for an air-glass boundary are plotted in Figure 2.

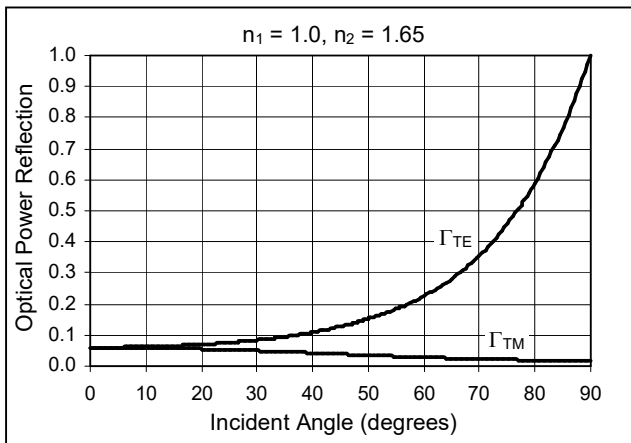


Figure 2. Power reflected versus incident angle

When coupling light into the single-mode optical fiber illustrated in Figure 1, the incident angles of interest are limited to $\theta_i < 10^\circ$ (for reasons that will be discussed in the next section). For this range of angles the reflection is approximately constant and independent of polarization. From equations (1), (2), and (3) we can calculate $R_{TE} \approx R_{TM} \approx 0.24$ for $\theta_i < 10^\circ$.

Since we are interested in the power of the reflected light (instead of the amplitude) we can calculate the power reflection coefficient for $\theta_i < 10^\circ$ as follows:

$$\Gamma = R_{TE}^2 = R_{TM}^2 = 0.24^2 = 0.0576 \quad (4)$$

where Γ is the power reflection coefficient and represents the ratio of the reflected power to the incident power. The transmitted power is just the difference between the incident power and the reflected power, so, for the boundary in Figure 1, approximately 94% of the incident power is transmitted across the air-glass boundary.

3 Total Internal Reflection

For the 94% of the light power that is transmitted across the air-glass boundary, there is yet another boundary that is encountered. This is the boundary between the core and the cladding of the optical fiber. The equations of the previous section apply equally to the core-cladding boundary, but with different indices of refraction. The index of

refraction for the incident medium (the core) is 1.65 versus 1.644 on the other side of the boundary (the cladding). This is illustrated in Figure 3.

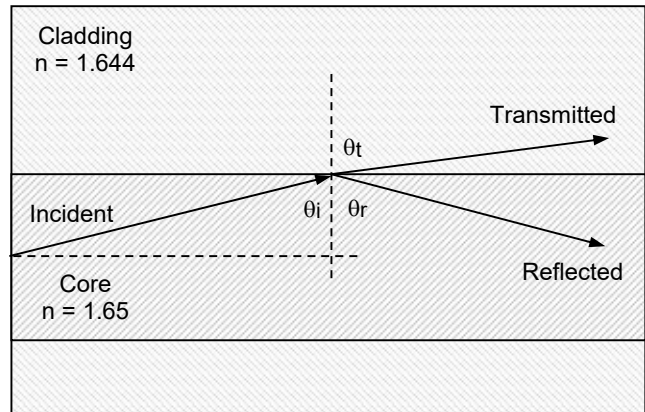


Figure 3. Light incident on core-cladding boundary

Since the cladding index of refraction is greater than the core index of refraction, the angle of transmitted light (θ_t) is greater than the angle of the incident light (θ_i). As the incident angle is increased, there is a point where the transmitted angle is 90° and no light is transmitted into the cladding. The incident angle that results in a transmitted angle of 90° is called the critical angle. The critical angle can be computed mathematically using equation (1) (Snell's law) as follows:

$$\theta_c = \sin^{-1} \left(\frac{n_2}{n_1} \sin 90^\circ \right) = \sin^{-1} \frac{n_2}{n_1} \quad (5)$$

where θ_c is the critical angle. For $n_1 = 1.65$ and $n_2 = 1.644$, equation (5) gives a critical angle of 85.1° . The power reflection coefficients for these indices of refraction can be calculated using the Fresnel equations [(2) and (3)]. These reflection coefficients are plotted in Figure 4.

From Figure 4 we can see that for incident angles greater than the critical angle 100% of the incident light is reflected, resulting in a condition called total internal reflection. Since the reflected angle is equal to the incident angle, the propagating light will repeatedly bounce back and forth between the core-cladding boundaries with the same angles. The process is repeated indefinitely, and the light propagates unimpeded along the length of the fiber.



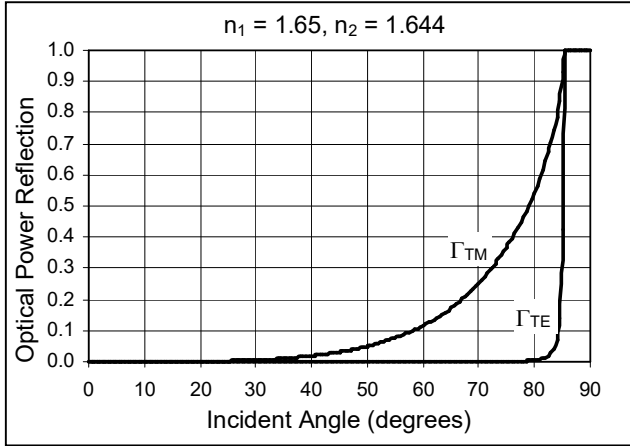


Figure 4. Power reflected versus incident angle

For incident angles less than the critical angle, some of the light is lost through transmission into the cladding and the rest is reflected back into the core of the fiber. The process is repeated, but each time the light hits the core-cladding boundary a fraction of the power is lost. Thus, for incident angles less than the critical angle, light propagates only a short distance in the core before it is totally lost to the cladding.

When coupling light into the optical fiber, we are generally interested only in the light that propagates, i.e. light that strikes the core-cladding boundary at an angle greater than the critical angle. Working back to the air-glass boundary, we see that the angle of the light entering the glass relative to the normal at the boundary (i.e., the angle labeled θ_t in Figure 1), must be less than $90^\circ - \theta_c$ for total internal reflection. Application of Snell's law to this condition yields the following equation for the acceptance angle of the fiber:

$$\theta_A = \sin^{-1}[n_{core} \sin(90^\circ - \theta_c)] \quad (6)$$

Using this equation for the example fiber gives an acceptance angle of 8.1° . (Note that the numerical aperture (NA) of the fiber is equivalent to the acceptance angle in units of radians.) An acceptance angle of 8.1° means that light striking the air-glass boundary at the core of the fiber will only propagate if the angle of incidence is less than 8.1° (0.14 radians).

4 Angular Divergence of the Laser Diode Output Power

In order to determine how much of the light output power from a laser diode will couple into the optical fiber, we need to know the angular divergence of its output power. This can be determined from the dimensions of the output aperture of the laser through the use of Fresnel/Fraunhofer diffraction theory¹ and Fourier optics².

For typical laser diodes, the active region (resonant cavity) has dimensions of 100-400 μm in length, 10-20 μm in width, and 0.1-0.3 μm in height^{3,4}. For example purposes, we will assume the output aperture is 10 μm wide (in the horizontal or x-dimension) and 0.2 μm high (in the vertical or y-dimension).

Fraunhofer diffraction theory is based on specific approximations that result in a convenient Fourier transform technique for determining the effect of an aperture on a beam of light. The Fraunhofer approximation becomes increasingly valid¹ as the distance from the aperture becomes greater than five to ten times the square of the maximum radius of the aperture divided by the wavelength (this is called the Fraunhofer distance). To use this technique we compute the product of the output aperture and the spatial intensity distribution of the light beam just inside the aperture. We then take the Fourier transform of the product and square the result⁵. This procedure can be written mathematically as:

$$P(f_x, f_y) = |\text{FT}[a(x, y) \times b(x, y)]|^2 \quad (7)$$

where, $P(f_x, f_y)$ is the angular distribution of the output power as a function of the spatial frequencies f_x and f_y , $\text{FT}[\]$ signifies the Fourier transform, $a(x, y)$ is the aperture function, and $b(x, y)$ is the spatial intensity distribution of the light beam.

The light output of a laser can be modeled as a Gaussian beam. For a Gaussian beam, the angular intensity profile can be represented by the Gaussian function $\exp[-\pi(x/w_x)^2] \exp[-\pi(y/w_y)^2]$, where w represents the aperture width in the x and y dimensions. This function has two unique properties: it's Fourier transform is also a Gaussian function; and a Gaussian beam maintains the same angular intensity profile in the Fresnel and Fraunhofer



regions (near and far field)¹. Using the properties of the Gaussian beam output of the laser diode along with equation (7), we can calculate the angular intensity profiles of the laser output power in the x-axis and y-axis.

Figures 5 and 6 are plots of the laser diode output power as a function of the divergence angle. These figures were generated using the Fourier transform technique described above. The mathematical derivation of these figures is detailed in the appendix at the end of this application note. The key point to observe is the inverse relationship between the angular divergence and the aperture dimensions. For example, the larger horizontal dimension results in a tighter angular intensity profile (Figure 5) while the smaller vertical dimension results in a wider angular intensity profile (Figure 6).

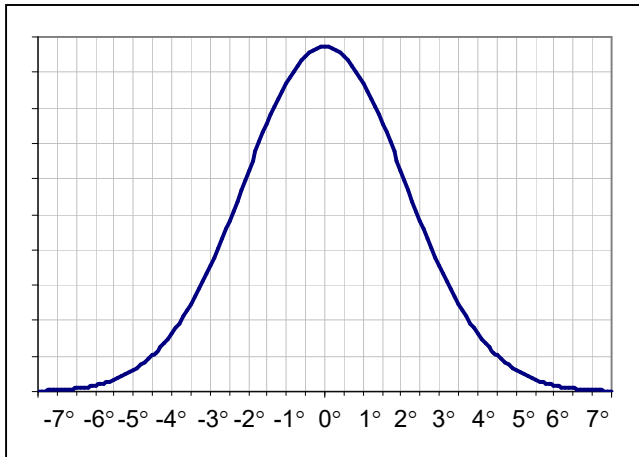


Figure 5. Gaussian angular intensity profile – horizontal dimension (x-axis)

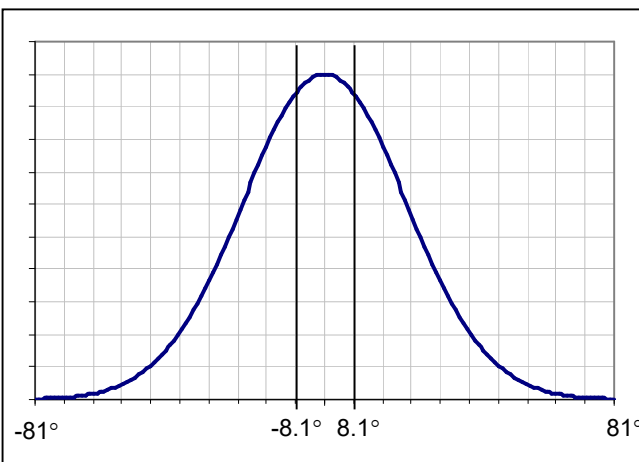


Figure 6. Gaussian angular intensity profile – vertical dimension (y-axis)

Recalling that the acceptance angle for the example optical fiber is 8.1°, we can see from Figures 5 and 6 that a butt-coupled optical fiber will accept most of the laser output power in the horizontal direction, but only a fraction of the power in the vertical dimension. We can calculate a reasonable estimate of the output power that will be accepted, by integrating the two angular intensity patterns over the range of acceptance angles and computing the product of the results, i.e.

$$P_A \approx \int_{-\theta_A}^{\theta_A} I_x(\theta_x) d\theta_x \times \int_{-\theta_A}^{\theta_A} I_y(\theta_y) d\theta_y \quad (8)$$

where P_A is the accepted power and $I(\theta)$ represents the angular intensity pattern. Application of equation (8) to the angular intensity patterns of Figures 5 and 6 (using numerical integration methods) results in $P_A \approx 31\%$ of the total output power.

5 Total Butt Coupling Losses

For the example analysis of this application note, we have calculated a reflection loss of 5.8% and an acceptance angle loss of 69%. Combining these losses, we can calculate the total fiber coupled power as $(1 - 0.0576)(1 - 0.69) = 29\%$ of the total laser output power.

In addition to the reflection and acceptance angle losses, there are a number of other possible losses that have not been addressed. These include losses due to: (1) imperfect cleaving of the optical fiber, (2) misalignment of the optical fiber, (3) laser output aperture dimensions larger than the fiber core (mismatch loss), and (4) intentional angling of the face of the optical fiber to reduce back reflections into the laser diode. All of these losses typically occur to some extent with butt coupling and will therefore reduce the fiber-coupled power beyond the figure calculated above. For example, some references report practical butt coupling efficiencies as low as 10%⁶.

6 Conclusions

We have demonstrated through analysis that the typical efficiency of butt coupling will be less than 29%. Clearly it is desirable to improve on this figure. There are many techniques that can be used to realize an improvement, including: (1) anti-reflection coatings and/or index matching gels to



reduce reflection losses, (2) improved alignment techniques, (3) lensed optical fibers, where the end of the fiber is specially shaped to improve the acceptance angle, and (4) lens systems that reshape the laser output for a better match to the fiber core. Using these and other techniques, coupling efficiencies as high as 87% have been reported⁷. Unfortunately these techniques can be complicated and expensive. Economical assembly to support competitive pricing may rule out all but the simplest methods. Thus, in many cases, butt coupling may be the only feasible method.



Appendix: Mathematical Details for Calculating the Angular Divergence of the Laser Output Power

For the maximum radius of the example aperture (5μm) and a wavelength of 1.31μm, the Fraunhofer distance is approximately 95 to 190μm. This means that equation (7) begins to be a good approximation at a distance of 95μm, and becomes a very accurate approximation for distances greater than 190μm. In practical butt coupling configurations, the cleaved end of the optical fiber is placed as close as possible to the output aperture of the laser diode, which is typically 10 to 20μm. Even though the distance between the aperture and the fiber does not meet the criteria for the Fraunhofer approximation, the criteria will be met after the light propagates a short distance down the fiber. Also, if we assume the laser output is a Gaussian beam then the Fraunhofer distance is irrelevant, since a Gaussian beam has the unique property that it maintains the same shape at all propagation distances¹. Thus, for practical purposes, we can assume that equation (7) is valid for a butt-coupled fiber.

We can write an expression for the two dimensional output aperture function in terms of the rectangular function $\text{rect}(x/w)$. This function has been defined to have a value of zero for $|x/w| > 0.5$, 0.5 for $|x/w| = 0.5$, and 1 for $|x/w| < 0.5$. We apply this function to the aperture by letting zero represent no light transmission and one represent full light transmission. Note that the $\text{rect}(x/w)$ function is

centered at $x = 0$ and it's width is equal to w . Using this function, we can write the following expression for the output aperture:

$$a(x, y) = \text{rect}\left(\frac{x\lambda d}{10\mu\text{m}}\right) \text{rect}\left(\frac{y\lambda d}{0.2\mu\text{m}}\right) \quad (9)$$

where λ is the wavelength of the light and d is the distance from the aperture.

The spatial distribution of the emitted laser light depends on the geometry of the resonator and on the shape of the active medium. If we assume that the mirrors at the ends of the resonant cavity are planar and perfectly parallel, then the laser output can be modeled as a plane wave, which we can express as $b(x,y) = 1$. Because of the difficulty in achieving sufficient alignment accuracy with planar mirrors, many laser designs use spherical mirrors. In this case, the laser output takes the form of a Gaussian beam⁸, which we can express as $b(x,y) = \text{Gauss}(x/w_x, y/w_y) = \exp[-\pi(x/w_x)^2] \exp[-\pi(y/w_y)^2]$. Regardless of whether we model the laser output as a plane wave or a Gaussian beam, the calculated angular divergence of the output power resulting from equation (7) will be approximately the same in the region of interest for the fiber coupling analysis. To illustrate this point, we will use equation (7) to calculate the result for both a plane wave and a Gaussian beam output.

For a plane wave, equation (7) can be solved as follows:

$$P(f_x, f_y) = \left| \text{FT} \left[1 \times \text{rect}\left(\frac{x\lambda d}{10}\right) \text{rect}\left(\frac{y\lambda d}{0.2}\right) \right] \right|^2 \\ = \frac{10}{\lambda d} \text{sinc}^2\left(\frac{10f_x}{\lambda d}\right) \times \frac{0.2}{\lambda d} \text{sinc}^2\left(\frac{0.2f_y}{\lambda d}\right) \quad (10)$$

where $\text{sinc}(f)$ is defined as $\sin(\pi f)/\pi f$.



For a Gaussian beam, equation (7) can be solved as:

$$P(f_x, f_y) = \left| \text{FT} \left[e^{-\pi \left(\frac{x}{10} \right)^2} e^{-\pi \left(\frac{y}{0.2} \right)^2} \times \text{rect} \left(\frac{x}{10} \right) \text{rect} \left(\frac{y}{0.2} \right) \right] \right|^2$$

$$\approx \frac{10}{\lambda d} e^{-2\pi \left(\frac{10 f_x}{\lambda d} \right)^2} \frac{0.2}{\lambda d} e^{-2\pi \left(\frac{0.2 f_y}{\lambda d} \right)^2} \quad (11)$$

Note that the result in equation (11) is obtained by observing that the rectangle function almost entirely contains the Gaussian function, resulting in a slightly truncated Gaussian function that closely approximates the original.

Figure 7 is a plot of both the $\text{sinc}^2(\cdot)$ function and the $\text{Gauss}^2(\cdot)$ functions. The plots are normalized to a spatial frequency of $\lambda d/w$, where λ is the wavelength of the light, d is the distance from the aperture, and w is the width of the aperture. In the region between $\pm \lambda d/w$ the results are similar for both functions. For purposes of this analysis, we will use the $\text{Gauss}^2(\cdot)$ function from this point forward in order to be consistent with results published in the literature⁹.

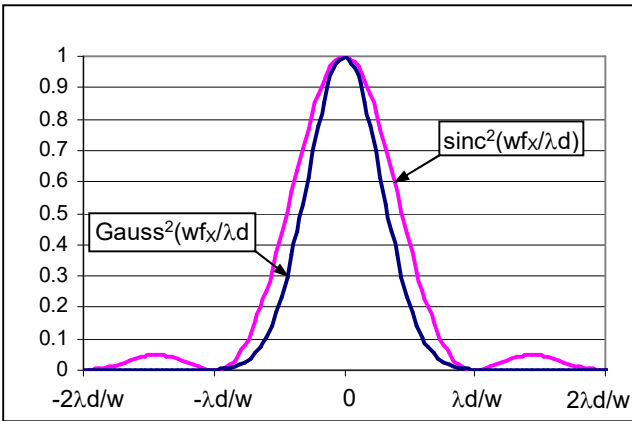


Figure 7. Normalized $\text{sinc}^2(\cdot)$ and $\text{Gauss}^2(\cdot)$ functions

Figures 5 and 6 are plots of the angular output intensity patterns along the x and y axis as calculated in equation (11). The divergence angles of the

intensity patterns are calculated by observing that the radial expansion of the intensity pattern divided by the propagation distance is equivalent to the tangent (in radians) of the divergence angle. For example, for the $\lambda d/w$ point on the intensity pattern the propagation distance is d , and therefore

$$\tan \theta = \frac{\lambda d}{w} \times \frac{1}{d} = \frac{\lambda}{w} \quad (12)$$

where θ is the angle of divergence.

¹ B.E.A. Saleh and M.C. Teich, *Fundamentals of Photonics*, New York, NY: John Wiley & Sons, Inc., 1991, pp. 128-134.

² J.W. Goodman, *Introduction to Fourier Optics*, San Francisco, CA: McGraw-Hill, 1968, pp. 57-70.

³ J.C. Palais, *Fiber Optic Communications, 4th Ed.*, Upper Saddle River, New Jersey: Prentice Hall, 1998, pp. 157.

⁴ P.E. Green, *Fiber Optic Networks*, Englewood Cliffs, New Jersey: Prentice Hall, 1993, pp. 160.

⁵ J.D. Gaskill, *Linear Systems, Fourier Transforms, and Optics*, New York, NY: John Wiley & Sons, 1978, pp. 375-380.

⁶ J.M. Senior, *Optical Fiber Communications: Principles and Practice, 2nd edition*, New York, NY: Prentice Hall, 1992, pp. 348.

⁷ H. Yoda and K. Shiraishi, "A New Scheme of a Lensed Fiber Employing a Wedge-Shaped Graded-Index Fiber Tip for the Coupling Between High-Power Laser Diodes and Single-Mode Fibers," *IEEE Journal of Lightwave Technology*, vol. 19, pp. 1910-1917, December 2001.

⁸ B.E.A. Saleh and M.C. Teich, *Fundamentals of Photonics*, New York, NY: John Wiley & Sons, Inc., 1991, pp. 513.

⁹ A. Ogura, S. Kuchiki, K. Shiraishi, K. Ohta, and I. Oishi, "Efficient Coupling Between Laser Diodes With a Highly Elliptical Field and Single-Mode Fibers by Means of GIO Fibers," *IEEE Photonics Technology Letters*, vol. 13, pp. 1191-1193, November 2001.